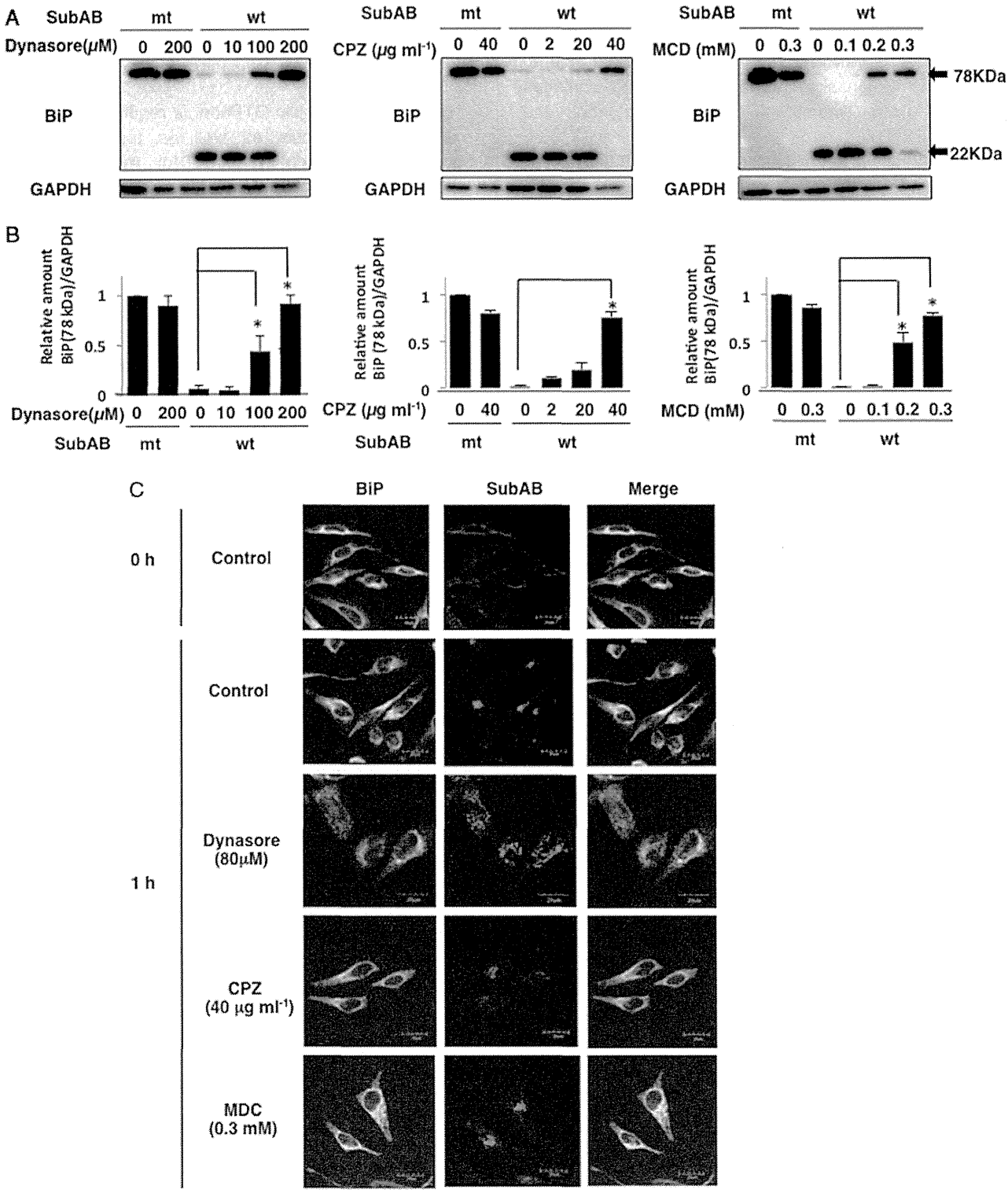

clathrin-knockdown cells, transferrin was mainly located at the cell surface, while SubAB was internalized (Fig. 1E). Further, to directly investigate if dynamin associates with SubAB uptake, we tested SubAB-mediated BiP cleavage in dynamin I/II knockdown by siRNA. As shown in Fig. 1F, dynamin I/II expression was significantly suppressed by the siRNA. Under this condition, SubAB-mediated BiP cleavage was not inhibited in dynamin I/II-

knockdown cells. We also monitored Alexa488-labelled transferrin as a positive control for dynamin-dependent endocytosis (Ferguson *et al.*, 2009) and Alexa555-labelled SubAB in dynamin I/II-knockdown cells. In control cells, both SubAB and transferrin were internalized and accumulated in the cytoplasm. In dynamin-knockdown cells, transferrin was not accumulated in the cytoplasm, however SubAB was internalized and accumulated (Fig. 1G). These findings are consistent with the hypothesis that internalization of SubAB into HeLa cells involves a clathrin- and dynamin-independent uptake pathway.

Caveolin does not contribute to SubAB uptake

A previous study showed that, in Vero cells, SubAB did not use a caveolin-dependent pathway for internalization (Chong *et al.*, 2008). Caveolae-mediated endocytosis is dependent on lipid rafts, and like other raft-mediated endocytic pathways, can be inhibited by cholesterol depletion. The effect of cholesterol depletion on SubAB entry was investigated using methyl-β-cyclodextrin (MβCD) and Filipin III, which extract cholesterol from membranes. As shown in Fig. 2A and B, 10 mM MβCD and 5 μg ml^{-1} Filipin III inhibited SubAB-mediated BiP cleavage and SubAB entry; Alexa555-conjugated CtxB uptake, used as a positive control, was also inhibited in the presence of the agents. In contrast, Alexa488-conjugated transferrin was used as a negative control; transferrin uptake into HeLa cells was not inhibited by these agents. These inhibitors did not directly inhibit SubAB-mediated BiP cleavage *in vitro* (Fig. 2C). Further, to examine the effect of caveolin on SubAB uptake, we tested SubAB-mediated BiP cleavage in caveolin1 and caveolin2 knockdown cells. As shown in Fig. 2D, both caveolin1 and caveolin2 expression was significantly suppressed by the siRNA. Under these conditions, SubAB-mediated BiP cleavage was not inhibited. These data indicate that internalization of SubAB is by a caveolin-independent and lipid raft-dependent pathway.

Filopodia are induced by SubAB

Macropinocytosis or the CLIC/GEEC pathway is initiated by changes in the dynamics of cortical actin in order to internalize particles or aqueous solutions via pseudopodia formation. Membrane ruffling occurs in response to directed actin polymerization near the plasma membrane, which lengthens into a roughly planar extension of the cell surface (Mercer and Helenius, 2009; Kumari *et al.*, 2010).

To assess the importance of actin microfilament rearrangement as the first step in SubAB entry, we examined whether SubAB treatment causes rearrangement of actin cytoskeleton in HeLa cells by staining with fluorescence-labelled phalloidin. We found that SubAB caused, in a time-dependent manner, a dramatic increase in number and length of filopodia (Fig. 3A). Number and surface density of SubAB-induced filopodia, quantified by confocal microscopy, was increased approximately fivefold (Fig. 3B), and mean length also increased twofold (Fig. 3C) compared with untreated cells. The surface areas of the cells did not decrease compared with cells not treated with SubAB, indicating that filopodia were not a consequence of cell retraction (Fig. 3D). Catalytically inactivated SubAB mutant (mSubAB) showed increased filopodia as well, revealing that these changes of filopodia formation are independent of SubAB-induced BiP cleavage (Fig. 3E). These results suggested that SubAB binding to cell surface increases filopodia as a trigger of entry into HeLa cells.

Fig. 1. Role of dynamin and clathrin during SubAB entry.
A. HeLa cells were pretreated with the indicated concentrations of Dynasore, CPZ or MDC, and then incubated with mSubAB (mt) or SubAB (wt) for 1 h. SubAB-induced BiP cleavage was determined by immunoblots. GAPDH served as a loading control. Experiments were repeated three times with similar results.
B. Quantification of uncleaved BiP (78 kDa) by mt or wt SubAB in the presence of the indicated inhibitors was performed by densitometry. Data are the means ± SD value from three independent experiments. $*P < 0.05$.
C. HeLa cells were pretreated with or without the indicated concentrations of inhibitors for 30 min, and then treated with Alexa555-labelled SubAB for 1 h. Cells were fixed and reacted with anti-BiP antibodies (green). A merged picture shows colocalization in HeLa cells. Bars represent 20 μm. Experiments were repeated two times with similar results.
D. HeLa cells were transfected with control (NC), clathrin siRNA or received no treatment, and cell lysates were subjected to immunoblotting with the indicated antibodies. GAPDH served as a loading control. Quantification by densitometry of the amounts of clathrin (192 kDa), with knockdown by the indicated siRNA. Clathrin siRNA-transfected cells were incubated with incubated with mSubAB (mt) or SubAB (wt) for the indicated times. SubAB-induced BiP cleavage was determined by immunoblots. GAPDH served as a loading control. Experiments were repeated three times with similar results. Data are the means ± SD from three separate experiments. $*P < 0.05$.
E. The indicated siRNA-transfected HeLa cells were incubated with Alexa555-labelled SubAB and Alexa488-labelled transferrin (Tf) for 1 h at 37°C. Bars represent 20 μm. Experiments were repeated two times with similar results.
F. Dynamin I/II siRNA-transfected cells were incubated with mSubAB (mt) or SubAB (wt) for 1 h. SubAB-induced BiP cleavage was determined by immunoblots with the indicated antibodies. Experiments were repeated three times with similar results.
G. The indicated siRNA-transfected HeLa cells were incubated with Alexa555-labelled SubAB or Alexa488-labelled transferrin (Tf) for 0.5 h at 37°C. Bars represent 20 μm. Experiments were repeated two times with similar results.

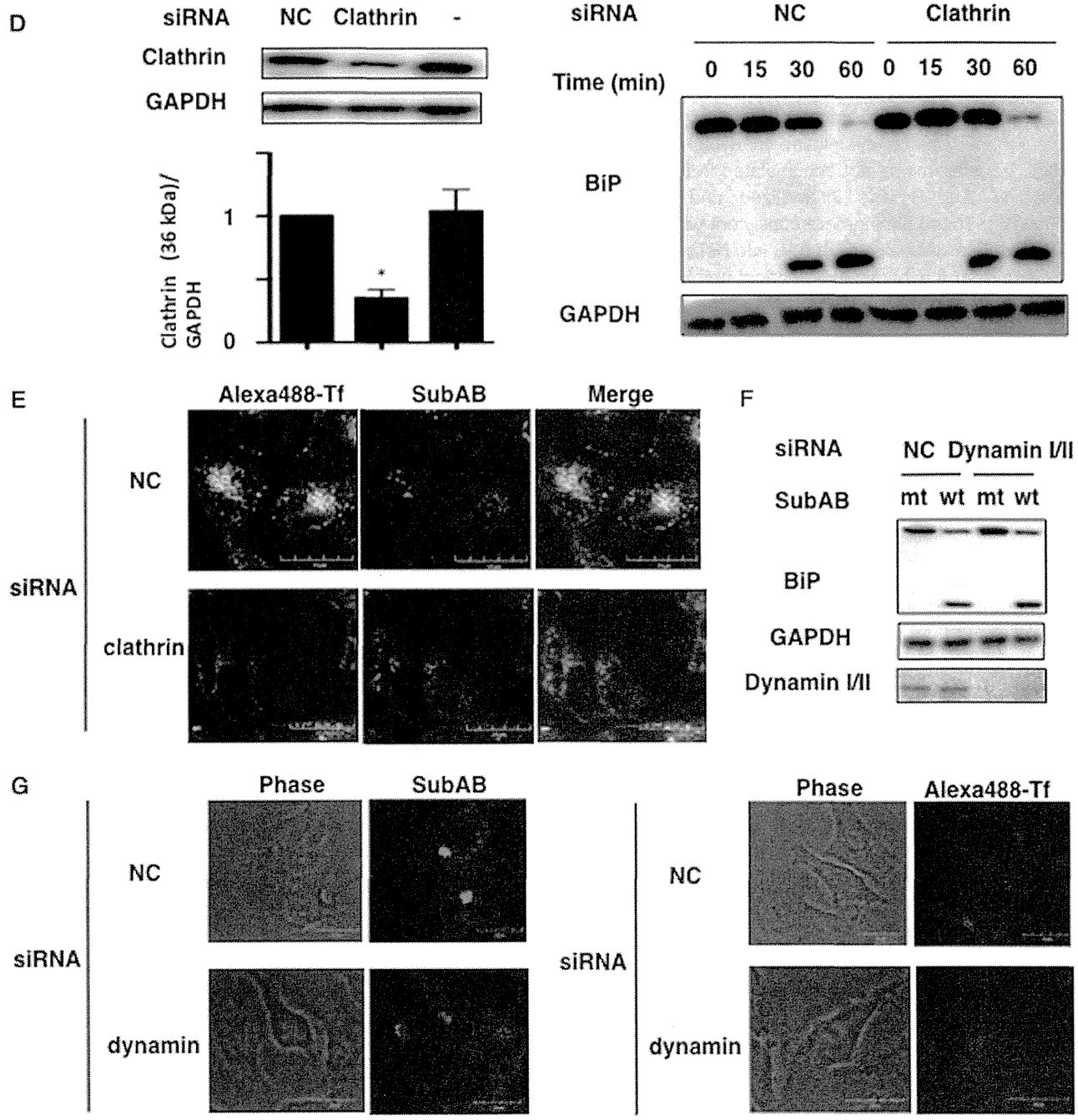

Fig. 1. *cont.*

SubAB entry is associated with Na^+/H^+ membrane exchange and stimulates uptake of fluid-phase markers

To further investigate the involvement of macropinocytosis on SubAB uptake, we examined the effect of 5-(N-ethyl-n-isopropyl)-amyloid (EIPA), a potent and specific inhibitor of Na^+/H^+ exchange activity, which leads to mild acidification of the cytosol, alters the subcellular localization of early and late endosomes, and possibly raises the luminal pH of mildly acidic organelles (Fretz *et al.*, 2006; Kalin *et al.*, 2010; Kumari *et al.*, 2010). A prior study showed that EIPA also blocked K^+ channels (Wang *et al.*, 1993). Upon pretreatment of HeLa cells with greater than 100 μM EIPA for 30 min, we noticed a dramatic inhibition of SubAB-induced BiP cleavage (Fig. 4A, upper panel). Confocal microscopy showed that EIPA pretreatment inhibited SubAB uptake (Fig. 4A, bottom panel and Fig. S1B). Furthermore, to confirm the effect of

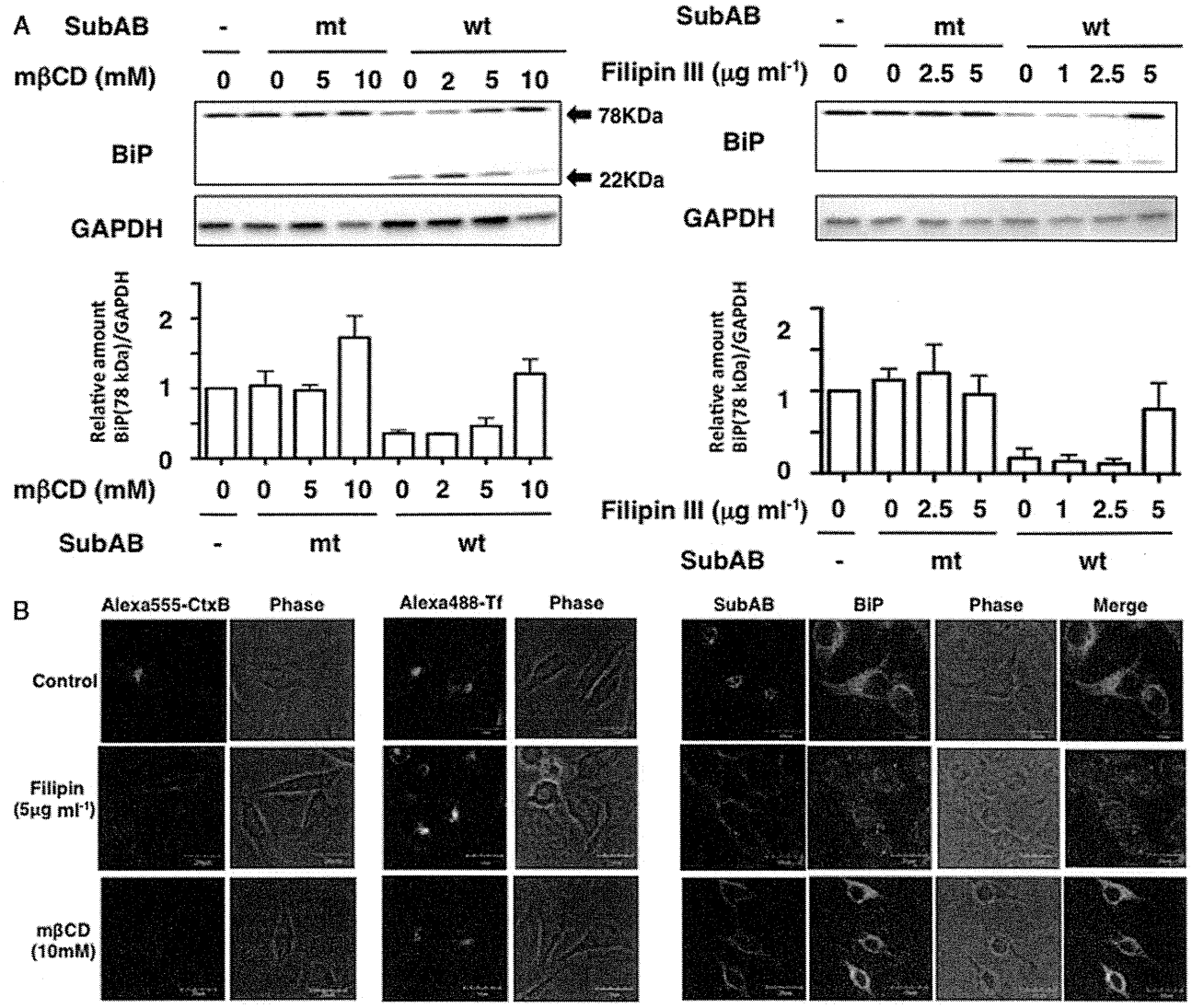

Fig. 2. SubAB uptake is lipid raft-dependent, not caveolin-dependent.
A. HeLa cells were pretreated with or without the indicated concentrations of caveolin inhibitors (i.e. Filipin III, MβCD) for 30 min and then incubated with mt or wt SubAB for 1 h. SubAB-mediated BiP cleavage was determined by immunoblots with the indicated antibodies. Experiments were repeated three times with similar results.
B. HeLa cells were pre-incubated with Filipin III (5 μg ml^{-1}), MβCD (10 mM) or DMSO as a control for 30 min at 37°C, and then cells were incubated with Alexa555-labelled CtxB (positive control), Alexa488-labelled transferrin (negative control) and Alexa555-labelled SubAB were incubated for 1 h at 37°C. Cells were fixed and observed by confocal microscopy. Bars represent 20 μm. Experiments were repeated two times with similar results.
C. The recombinant hamster BiP (0.1 μg per 10 μl) was incubated with SubAB (20 ng per 10 μl) in the presence or absence of Filipin III (5 μg ml^{-1}), MβCD (10 mM) or DMSO as a control for 1 h at 37°C, and then cleaved BiP was detected with anti-BiP antibody by Western blotting as described in *Experimental procedures*. Experiments were repeated two times with similar results.
D. Control (NC), caveolin1 (Cav1) and caveolin2 (Cav2) siRNA-transfected cells were incubated with SubAB for the indicated times at 37°C. The expression levels of Cav1 and Cav2 and SubAB-mediated BiP cleavage were determined by immunoblots with the indicated antibodies. Experiments were repeated three times with similar results.

EIPA activity on SubAB uptake, we used media with or without Na^+ and/or K^+ as described previously (Koivusalo *et al.*, 2010). In Na^+-rich media condition, SubAB induced BiP cleavage and Alexa555-labelled SubAB was internalized by cells. In K^+-rich media, Alexa555-labelled SubAB was internalized similar to that seen in Na^+-rich media, but SubAB-mediated BiP cleavage was significantly inhibited. When both Na^+ and K^+ were replaced by N-methyl-glucosamine (NMG^+), we observed inhibition of SubAB-induced BiP cleavage and its accumulation in cells similar to what was seen in EIPA-treated cells, suggesting that SubAB entry occurs through an

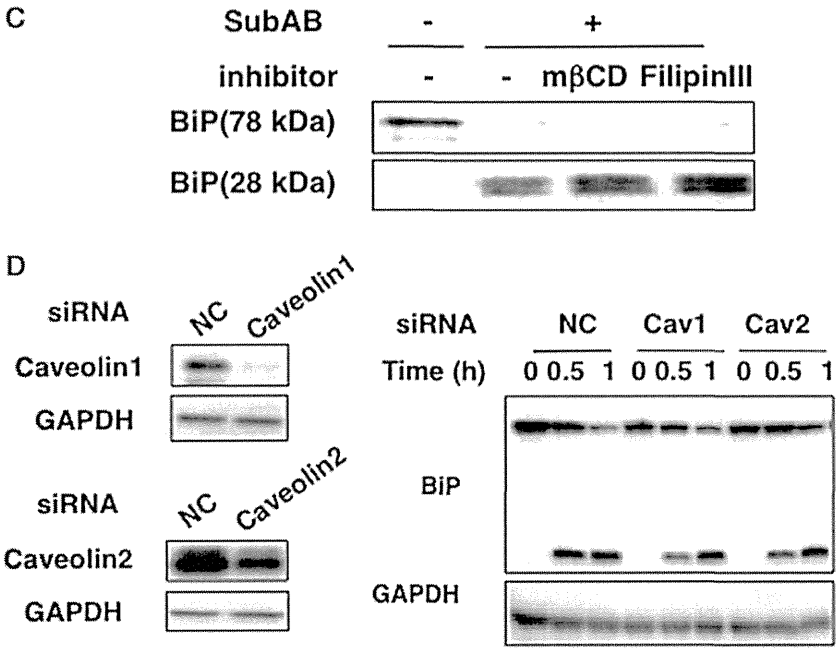

Fig. 2. *cont.*

EIPA-sensitive pathway (Fig. 4B). We next examined the effect of bafilomycin A1 (Baf A1), which acts on the vacuolar-type H (+)-ATPase, thus preventing endosomal acidification (Williamson and Neale, 1994), on SubAB uptake. As shown in Fig. 4C, Baf A1 pretreatment decreased SubAB-mediated BiP cleavage in a dose-dependent manner. In further support of this result, we monitored Alexa555-labelled SubAB uptake in the presence or absence of Baf A1 by confocal microscopy. In the presence of Baf A1, SubAB internalized into the cytoplasm, however its accumulation was significantly decreased compared with control cells (Fig. 4C, bottom).

Since activation of macropinocytosis or the CLIC/GEEC pathway induces a transient increase in uptake of dextran, a fluid phase marker (Dharmawardhane *et al.*, 2000; Nonnenmacher and Weber, 2011), we next investigated dextran uptake during SubAB entry. We visualized the uptake of FITC-labelled dextran (fDx) in the presence or absence of SubAB by confocal microscopy (Fig. 4D). Notably, most fDx puncta were colocalized with SubAB in a subcellular fraction and fDx uptake significantly increased in the presence of SubAB (Fig. 4E).

Association of PI3K and Ca^{2+} with SubAB uptake

Falcon *et al.* have shown in dendritic cells that not only PI3K activity, but also Ca^{2+} is required for macropinocytosis (Falcone *et al.*, 2006). Jiang and Chen (2009) also reported that dynamin-independent endocytosis is tightly regulated by intracellular Ca^{2+}. PI3K inhibitors (e.g. LY294002, wortmannin) blocked SubAB uptake, in a dose-dependent manner (Fig. 5A). Next, we investigated whether SubAB uptake pathway is dependent on extracellular or intracellular Ca^{2+} signalling. HeLa cells were incubated with mSubAB or SubAB in the presence or absence of EGTA; no significant difference was observed in BiP cleavage. The Ca^{2+} ionophore, ionomycin, which allows Ca^{2+} influx from the ER and increases intracellular Ca^{2+} concentration, slightly increased, in a dose-dependent manner, the cleaved form of BiP (28 kDa) and decreased the amount of mature BiP (78 kDa) observed in the presence of SubAB. Blocking intracellular Ca^{2+} by pretreatment with Ca^{2+} chelator BAPTA-AM significantly inhibited SubAB-mediated BiP cleavage (Fig. 5B). We further monitored SubAB internalization by using Alexa555-labelled or biotin-labelled SubAB in the presence or absence of LY294002, wortmannin and BAPTA-AM (Figs 5C and S1B). Following treatment with wortmannin and BAPTA-AM, SubAB was mainly located on the cell surface and entry into the cells was inhibited. After LY294002 treatment, we observed SubAB puncta in the cells, which was different from the appearance in untreated cells as shown in Fig. 1C.

PAK1 does not participate in SubAB uptake

The serine/threonine kinase p21-activated kinase (PAK) is also an important protein of macropinocytosis (Dharmawardhane *et al.*, 2000). Treatment of HeLa cells with an allosteric PAK1 inhibitor IPA-3 inhibited SubAB-mediated BiP cleavage (Fig. 6A). Previous studies showed that the macropinocytosis pathway was

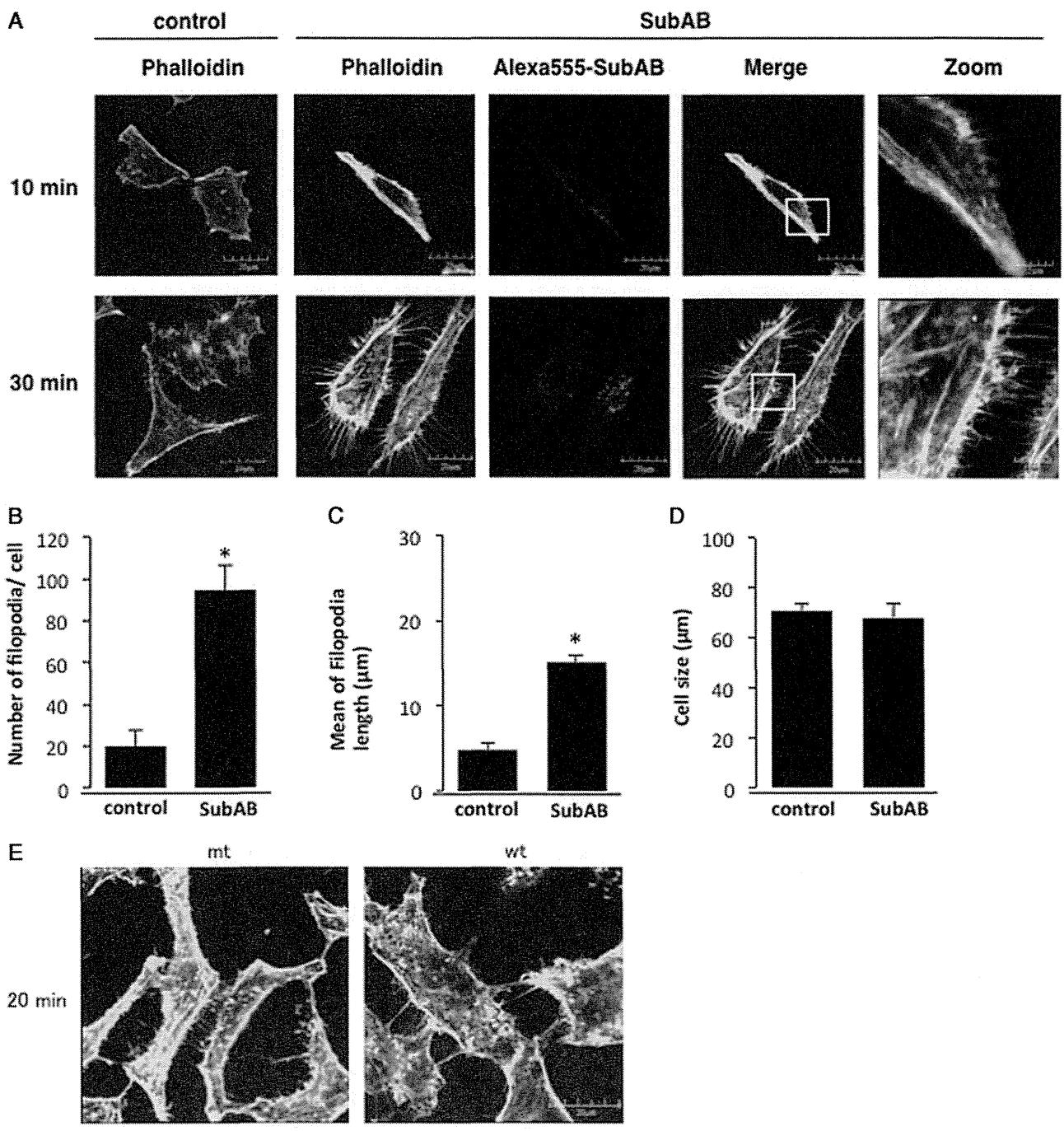

Fig. 3. SubAB-induced the extension of filopodia.

A. HeLa cells were incubated with or without Alexa555-labelled SubAB for 10 or 30 min at 37°C, fixed, and stained with F-actin by anti-stain™ 488 fluorescent phalloidin (PHDG1) antibody (green). A merged picture shows colocalization in HeLa cells. Bars represent 20 μm. Experiments were repeated three times with similar results.

B–D. Cells, treated as in (A), were subjected to quantitative measurements, including the number of filopodia per cell (B), filopodia length (C), and 2D cell size (D). Data are the means ± SD from three separate experiments, which involved quantifying two cells chosen at random. $^*P < 0.05$.

E. HeLa cells were incubated with mt or wt SubAB for 20 min at 37°C, fixed, and stained for F-actin by anti-stain™ 488 fluorescent phalloidin (PHDG1) antibody (green). Picture shows that both mt and wt SubAB induced filopodia. Experiments were repeated three times with similar results.

Fig. 4. SubAB uptake is dependent on Na^+/H^+ membrane exchanger in HeLa cells.
A. Cells were pretreated with or without the indicated concentrations of EIPA for 30 min and then incubated with mt or wt SubAB for 1 h. SubAB-induced BiP cleavage was determined by Western blot analysis. GAPDH served as a loading control. Experiments were repeated three times with similar results (Top panel). HeLa cells were pre-incubated with 100 μM EIPA or DMSO as a control for 30 min at 37°C, and Alexa555-labelled SubAB were incubated for 1 h at 37°C. Cells were fixed and observed by confocal microscopy. Bars represent 20 μm. Experiments were repeated two times with similar results (bottom panel).
B. Cells were pre-incubated with Na^+-rich (Na^+), K^+-rich (K^+) or NMG^+-rich (NMG^+) buffer for 30 min and then incubated with mt or wt SubAB for 1 h. SubAB-induced BiP cleavage was determined by Western blot analysis. GAPDH served as a loading control. Experiments were repeated two times with similar results (Top, left panel). Quantification of uncleaved BiP (78 kDa) following incubation with mt or wt SubAB in the presence of Baf A1 was performed by densitometry. Data are the means ± SD from three independent experiments (Top, right panel). $^*P < 0.05$. HeLa cells were pre-incubated with EMEM as a control and the indicated buffer for 30 min at 37°C, and Alexa555-labelled SubAB was added for 1 h at 37°C. Cells were fixed and analysed by confocal microscopy. Bars represent 20 μm. Experiments were repeated two times with similar results (bottom panel).
C. HeLa cells were pretreated with the indicated concentration of Baf A1 for 30 min and then incubated with mt or wt SubAB for 1 h. SubAB-induced BiP cleavage was determined by Western blot analysis as described above (left panel). Quantification of uncleaved BiP (78 kDa) following incubation with mt or wt SubAB in the presence of Baf A1 was performed by densitometry. Data are the means ± SD from three independent experiments (right panel). $^*P < 0.05$. HeLa cells were pre-incubated with 0.5 μM Baf A1 or control as shown in Fig. 1C for 30 min at 37°C, and then incubated with Alexa555-labelled SubAB for 1 h at 37°C. Cells were fixed and observed by confocal microscopy. Bars represent 20 μm. Experiments were repeated two times with similar results (bottom panel).
D. SubAB stimulates fluid-phase macropinocytosis in HeLa cells. SubAB was bound on ice to cells, which were then incubated at 37°C for 1 h, with exposure to FITC-dextran (fDx) during the last 10 min; results were analysed by confocal microscopy. A merged picture demonstrated that SubAB treatment enhanced fDx uptake. Transiently both SubAB and fDx were colocalized. A merged picture shows colocalization. Bars represent 20 μm. Experiments were repeated three times with similar results.
E. Quantification of fDx(dot) in cells was determined by confocal microscopy ($n = 10$). Data are the means ± SD from three independent experiments. $^*P < 0.05$.

inhibited by 20~80 μM IPA-3 (de Vries *et al.*, 2011; Sanchez *et al.*, 2012; Krzyzaniak *et al.*, 2013). Next, we examined the effect of IPA-3 on SubAB-mediated BiP cleavage *in vitro*. Interestingly, we found that IPA-3 was able to inhibit SubAB activity (Fig. 6B). By confocal microscopy, we observed that IPA-3 treatment inhibited SubAB uptake and its accumulation in cells, with the toxin localized at dots on the cell surface (Fig. 6C). We next examined the effect of PAK1 knockdown on SubAB-mediated BiP cleavage. Although PAK1 was significantly suppressed, BiP cleavage by SubAB was not inhibited in these cells, suggesting that SubAB uptake was independent of the PAK1 pathway (Fig. 6D).

SubAB entry involves the actin cytoskeleton and detergent-resistant membranes

As described above, macropinocytosis requires actin membrane protrusion that develops into vesicles, termed macropinosomes (Wadia *et al.*, 2004). We further investigated the contribution of F-actin to the internalization of SubAB by treating the cells with cytochalasin D (CytD), which is known to induce depolymerization of F-actin. After pre-incubation with CytD (1, 5, 10 μM), SubAB-induced BiP cleavage was significantly suppressed (Fig. 7A) and Alexa555-labelled SubAB was predominantly localized on the cell surface (Fig. 7B). Consistent with these results, we observed that uptake of biotin-labelled SubAB was inhibited by Cyt D (Fig. S1B). We next examined if cholesterol in cells is necessary for SubAB translocation. Interestingly in live cells, most internalized Alexa555-labelled SubAB was resistant to cold Triton X-100 extraction. In contrast, Alexa488-labelled Tf was almost completely extracted (Fig. 8). These data suggest that SubAB uptake is involved in actin cytoskeleton and the internalized SubAB compartment is associated with cholesterol-rich DRMs.

Discussion

Eukaryotic cells utilize different types of endocytosis, which is divided into two main classes, those involving mainly fluid solutes (pinocytosis) and those where large particles are internalized (phagocytosis) (Mercer and Helenius, 2009). Pathogens or viruses can cross the physical barrier represented by the plasma membrane and pass through the underlying cortical matrix (Gruenberg and van der Goot, 2006). In Vero cells, SubAB was internalized by clathrin-dependent endocytosis (Chong *et al.*, 2008). In HeLa cells, however, clathrin knockdown did not entirely suppress SubAB-induced BiP cleavage, suggesting that SubAB uses other pathways to enter HeLa cells. In this report, we assessed the participation of other pathways in SubAB uptake.

Dynamin is a high molecular weight GTPase, which is involved in scission of newly formed endocytic vesicles at the plasma membrane (Henley *et al.*, 1998; Lajoie *et al.*, 2009). In this report, we show that SubAB-induced BiP cleavage was suppressed only by a high concentration of Dynasore, a dynamin inhibitor, however endocytosis was not suppressed. Furthermore, clathrin inhibitors, CPZ and MCD, at high concentrations, also inhibited SubAB-induced BiP cleavage, but SubAB uptake was not inhibited. Mesaki *et al.* reported that a

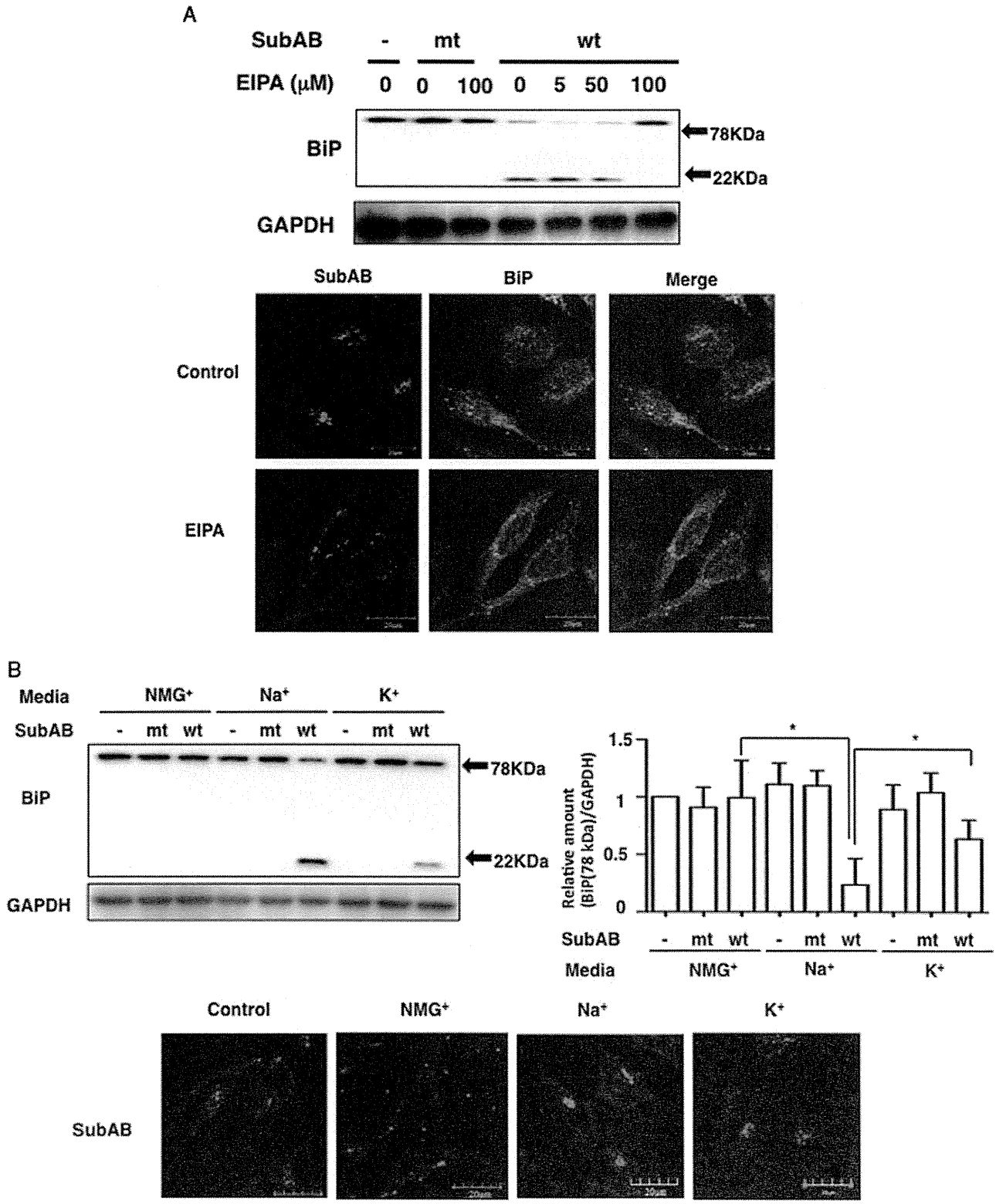
A
SubAB
-
mt
wt
EIPA (μM)
0
0
100
0
5
50
100
BiP
78KDa
22KDa
GAPDH
SubAB
BiP
Merge
Control
EIPA
B
Media
NMG+
Na+
K+
SubAB
-
mt
wt
BiP
78KDa
22KDa
GAPDH
Relative amount (BiP(78 kDa)/GAPDH)
1.5
1
0.5
0
*
*
Control
NMG+
Na+
K+
SubAB

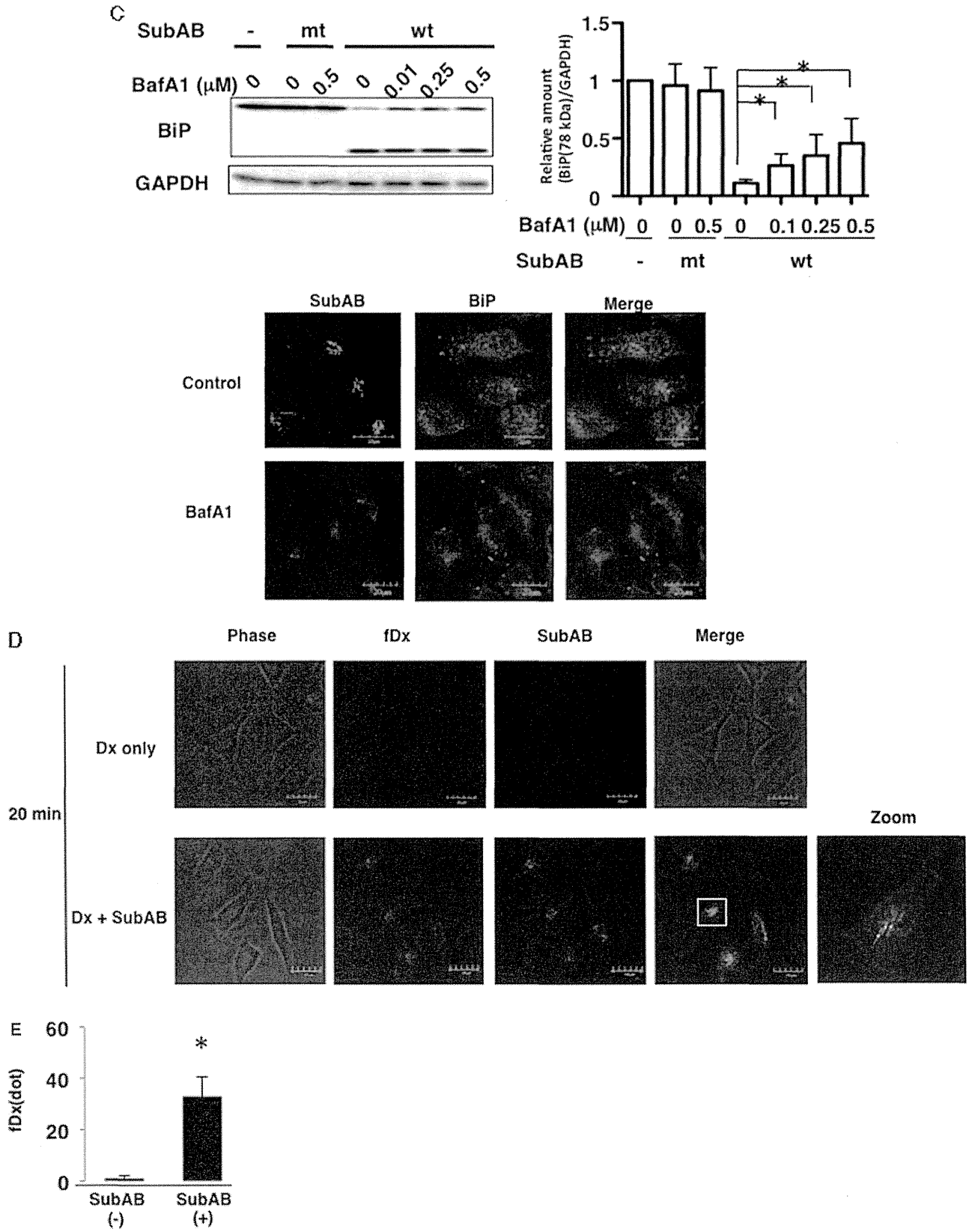
C
SubAB
-
mt
wt
BafA1 (μM)
0
0
0.5
0
0.01
0.25
0.5
BiP
GAPDH
Relative amount (BiP(78 kDa)/GAPDH)
1.5
1
0.5
0
BafA1 (μM) 0 0 0.5 0 0.1 0.25 0.5
SubAB - mt wt
SubAB
BiP
Merge
Control
BafA1
D
Phase
fDx
SubAB
Merge
Dx only
20 min
Dx + SubAB
Zoom
E
fDx(dot)
60
40
20
0
SubAB (-)
SubAB (+)

Fig. 4. *cont.*

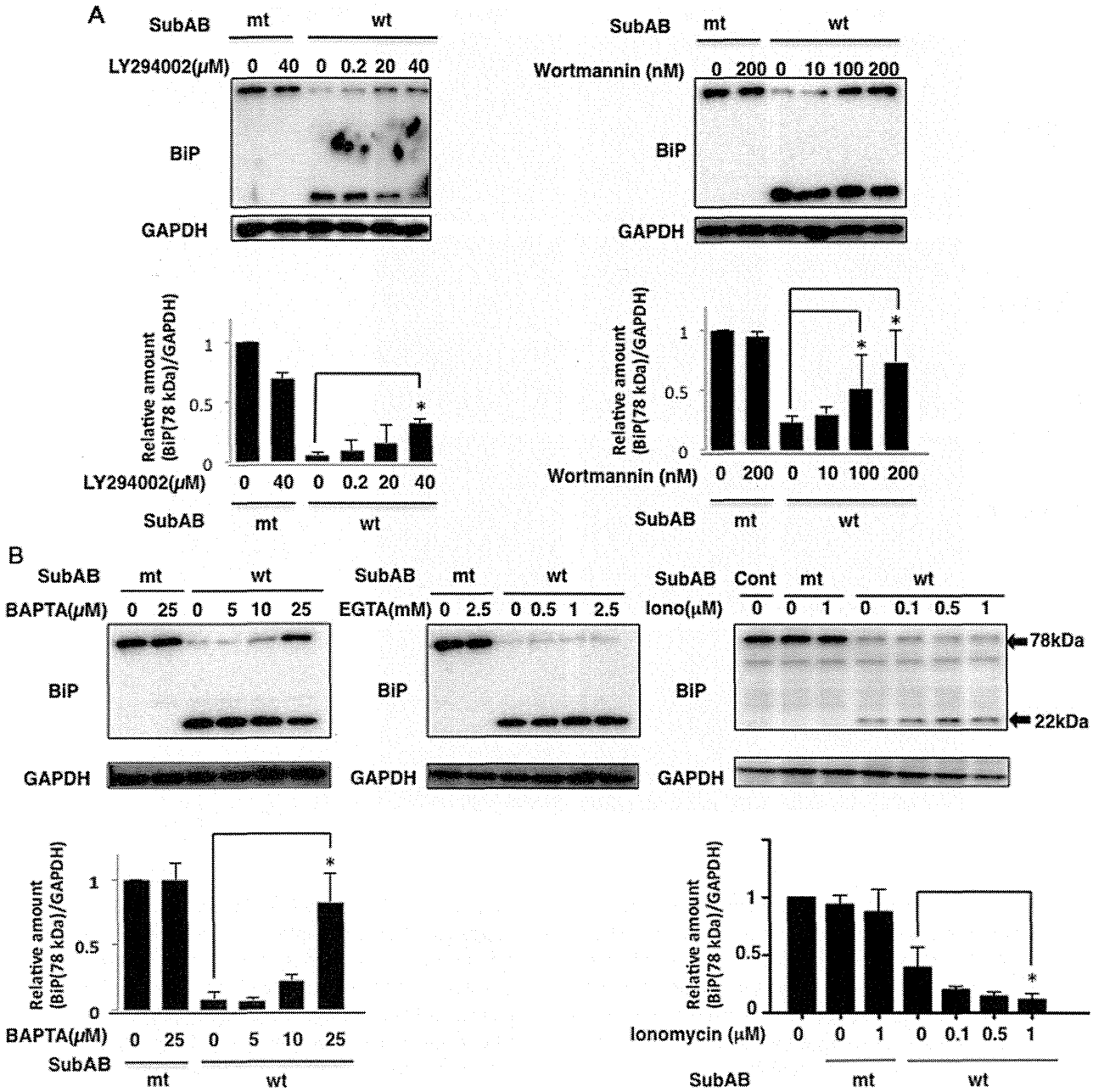

Fig. 5. Effect of PI3K inhibitors and Ca^{2+} on SubAB uptake by HeLa cells.
A. SubAB entry was determined by BiP cleavage using Western blot in cells pretreated with the indicated concentrations of LY294002 or wortmannin.
B. Cells were pretreated with the indicated concentrations of BAPTA-AM, EGTA or ionomycin, and then incubated with mt or wt SubAB for 45 min at 37°C. Analysis was performed by Western blot using anti-BiP and anti-GAPDH antibodies. Experiments were repeated three times with similar results. Quantification of uncleaved BiP (78 kDa) following incubation with mt or wt SubAB in the presence of the indicated inhibitors was performed by densitometry. Data are the means ± SD from three independent experiments. $^*P < 0.05$.
C. HeLa cells were pretreated with or without the indicated concentrations of inhibitors for 30 min and then treated with Alexa555-labelled SubAB for 1 h. Cells were fixed and reacted with anti-BiP antibodies (green). A merged picture shows colocalization in HeLa cells. Bars represent 20 μm. Experiments were repeated two times with similar results.

high concentration of Dynasore (400 μM) blocked tubular endosome fission, early endosomal intraluminal acidification, endosomal motility along microtubules and perinuclear localization (Mesaki *et al.*, 2011). Thus, these intracellular effects of Dynasore interfered with SubAB trafficking. In addition, Dynamin I/II gene silencing by siRNA did not suppress SubAB-mediated BiP cleavage. Furthermore, we demonstrated here that SubAB-

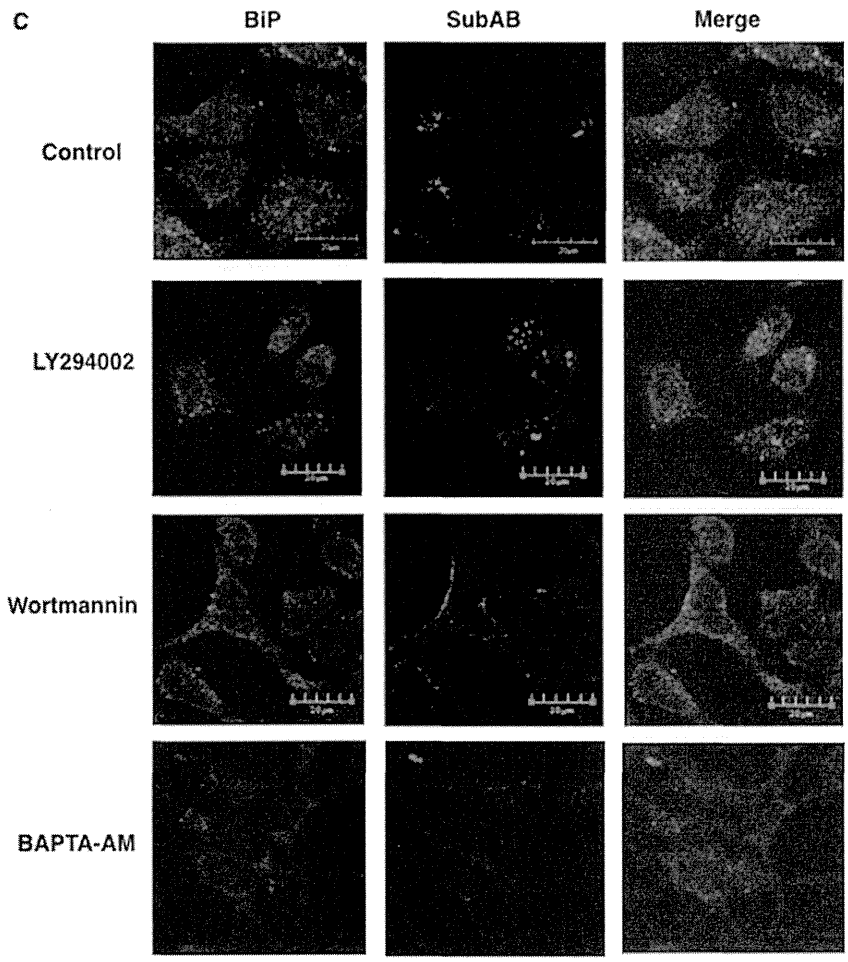

Fig. 5. *cont.*

mediated BiP cleavage was not inhibited in caveolin 1- and 2-knockdown cells. Recently, Park *et al.* developed dynamin triple knockout cells, which will be useful tools for the further exploration of dynamin-dependent processes and the exclude side-effects of dynamin inhibitors (Park *et al.*, 2013). Taken together, these data suggest that SubAB uptake occurs by clathrin-, dynamin I/II-, and caveolin-independent pathways.

Cholera toxin, VacA toxin from *Helicobacter pylori* and adeno-associated viruses (AAVs) serve as markers for the clathrin-independent carriers/GPI-anchored-protein-enriched endosomal compartment (CLIC/GEEC) pathway (Howes *et al.*, 2010; Nonnenmacher and Weber, 2011; Boquet and Ricci, 2012). The CLIC/GEEC pathway is independent of dynamin, and required actin cytoskeleton dynamics and cholesterol microdomains (Doherty and McMahon, 2009). A previous study showed that Filipin III inhibits caveolae-mediated uptake by binding to 3β-hydroxysterol, a major component of glycolipid microdomains and caveolae (Orlandi and Fishman, 1998). We show here that SubAB uptake is sensitive to cytochalasin D, Filipin III and mβCD (Figs 2, 7 and S1B), suggesting SubAB uptake is associated with actin cytoskeleton dynamics and lipid rafts. Furthermore, we observed that the internalized SubAB compartment was associated with DRMs, suggesting that SubAB is localized to the cellular cholesterol-containing endocytic vesicles. Our findings indicate that SubAB uptake is affected by actin cytoskeleton dynamics and cholesterol plays an essential role in SubAB internalization and intracellular trafficking.

As described above, viruses use macropinocytosis and the CLIC/GEEC pathway for productive infection (Mercer and Helenius, 2009; Nonnenmacher and Weber, 2011). Activation of macropinocytosis and CLIC/GEEC involves significant cell-wide membrane ruffling, mediated by activation of actin filaments (Kumari *et al.*, 2010; Sanchez *et al.*, 2012). These structures may have different shapes: filopodia, circular-shaped membrane extrusions and large membrane extrusions (Doherty and McMahon, 2009). Mercer and colleagues reported that vaccinia virus could induce transient macropinocytosis followed by endocytic

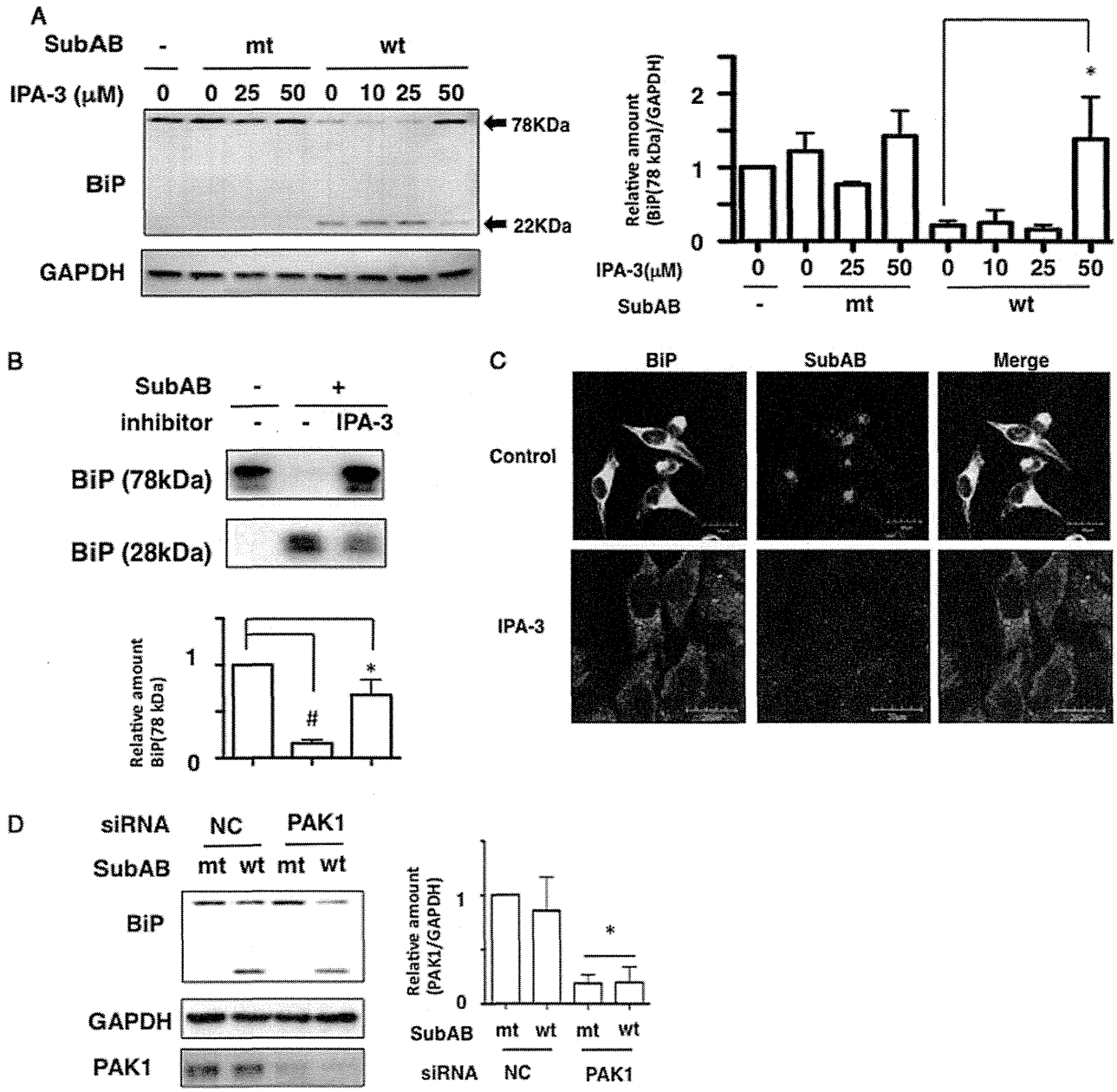

Fig. 6. Effects of IPA-3 on SubAB uptake by HeLa cells.

A. HeLa cells were pretreated with the indicated concentrations of IPA-3 for 30 min, and then cells were incubated with mt or wt SubAB for 1 h and effects determined by Western blot as described above (left panel). Quantification of uncleaved BiP (78 kDa) following incubation with mt or wt SubAB in the presence of the indicated inhibitors was performed by densitometry (right panel). Data are the means ± SD from three separate experiments. $^{*}P < 0.05$.

B. Recombinant hamster BiP was incubated with SubAB with or without IPA-3 (50 μM) for 1 h at 37°C as described in *Experimental procedures*. Data are the means ± SD from five separate experiments. $^{\#}P < 0.05$, $^{*}P < 0.03$.

C. Cells were pretreated with 50 μM IPA-3 for 30 min and then incubated with Alexa555-labelled SubAB for 1 h at 37°C. Cells were imaged by confocal microscopy for colocalization of SubAB (red) with BiP (green) as described in *Experimental procedures*. Bars represent 20 μm. Experiments were repeated two times with similar results.

D. The indicated siRNA-transfected cells were incubated with mt or wt SubAB for 1 h and effects determined by Western blot as described above (left panel). Quantification by densitometry of the amounts of PAK1 with knockdown by siRNA (right panel). Data are the means ± SD from three separate experiments. $^{*}P < 0.05$.

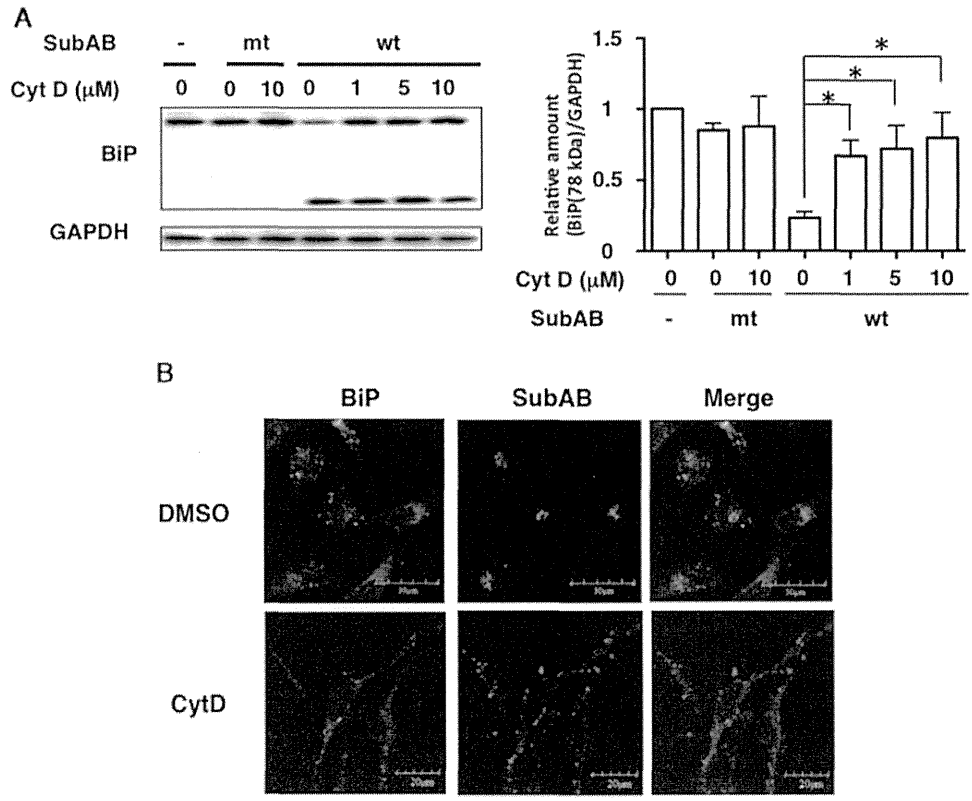

Fig. 7. SubAB entry involves the actin cytoskeleton.
A. HeLa cells were pretreated with the indicated concentrations of cytochalasin D (Cyt D) for 30 min, and then cells were incubated with mt or wt SubAB for 1 h and effects determined by Western blot as described above (left panel). Quantification of uncleaved BiP (78 kDa) following incubation with mt or wt SubAB in the presence of the indicated inhibitors was performed by densitometry (right panel). Data are the means ± SD from three separate experiments. $^*P < 0.05$.
B. Cells were pretreated with 10 μM Cyt D or control DMSO for 30 min and then incubated with Alexa555-labelled SubAB for 1 h at 37°C. Cells were imaged by confocal microscopy for colocalization of SubAB (red) with BiP (green) as described in *Experimental procedures*. Bars represent 20 or 30 μm. Experiments were repeated three times with similar results.

internalization to enter target cells, with rapid formation of filopodia (Mercer *et al.*, 2010). Based on our data, SubAB treatment caused a dramatic increase in number and length of filopodia, similar to that seen with vaccinia virus. We also observed that mutant SubAB increased these filopodia, indicating that the interaction between SubAB and target cells caused the rapid formation of filopodia; SubAB-induced BiP cleavage was not involved.

Previous studies have suggested that the signalling cascade that activates blebbing and subsequent macropinocytosis of virus involves several kinases (Mercer and Helenius, 2008; Mercer *et al.*, 2010), in addition to the Na^+/H^+ exchanger and PI3K. To further investigate if other kinases were participated in SubAB entry, we examined the effect of Rottlerin on SubAB entry and BiP cleavage. As shown in Fig. S2A, SubAB-mediated BiP cleavage was inhibited by Rottlerin in a dose-dependent manner. We next monitored Alexa555-labIled SubAB uptake in the presence or absence of Rottlerin by confocal microscopy. In the presence of Rottlerin, SubAB localized on the cell surface and did not enter HeLa cells (Fig. S2B). However, a recent study showed that Rottlerin, a typical macropinocytosis inhibitor, did not directly block PKCδ activity but activated multiple pathways via mitochondria uncoupling (Soltoff, 2007). As shown in above, SubAB uptake was completely inhibited by 40 μM Rottlerin. However, we detected SubAB-mediated BiP cleavage in PKCδ-knockdown cells (Fig. S2C), indicating that PKCδ was not involved in SubAB internalization and a side-effect of Rottlerin may be inhibition of SubAB uptake.

We investigated whether the inhibitors used in this study directly suppressed SubAB-induced BiP cleavage by using purified hamster BiP *in vitro*. As shown in Fig. S3, inhibitors used in this study except for IPA-3 did not directly inhibit BiP cleavage by SubAB. IPA-3 inhibited SubAB-mediated BiP cleavage *in vivo* and *in vitro*, and both SubAB uptake and its accumulation in cells were significantly decreased, suggesting that a PAK1-dependent pathway is involved in SubAB entry. Previous

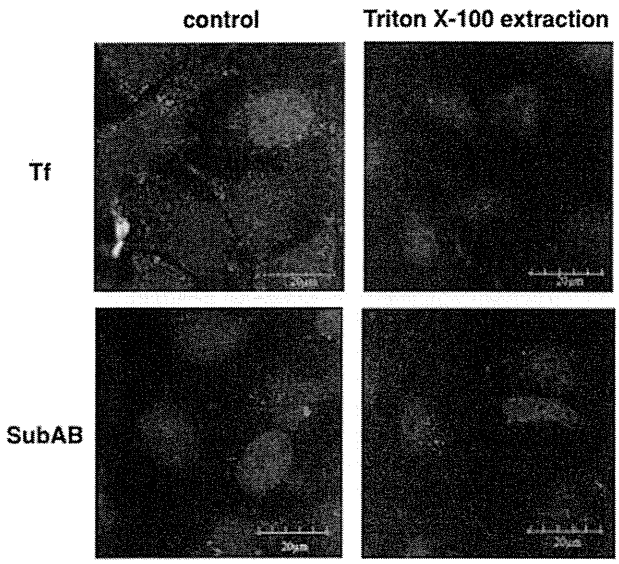

Fig. 8. Internalized SubAB associated with DRMs. HeLa cells were incubated with Alexa488-labelled Tf (green) and Alexa555-labelled SubAB (red) for 30 min, were subjected to cold Triton X-100 extraction and imaged by confocal microscopy of SubAB (red), Tf (green) and DAPI (blue) as described in *Experimental procedures*. Bars represent 20 μm. Experiments were repeated three times with similar results.

studies demonstrated that IPA-3 binds covalently to the PAK1 regulatory domain and prevents binding to the upstream activator Cdc42 (Viaud and Peterson, 2009). PAK1 is known to be an important factor of macropinocytosis (Dharmawardhane *et al.*, 2000). In this experiment, we could not clear how IPA-3 inhibits SubAB-mediated BiP cleavage *in vitro*. It is conceivable that IPA-3 directly associated with SubAB or SubAB recognition site of BiP, resulting in a block in SubAB-mediated BiP cleavage. However, SubAB-mediated BiP cleavage was not suppressed following PAK1 knockdown, suggesting that SubAB uptake occurs by a PAK1-independent pathway.

SubAB was discovered in non-O157, LEE-negative Shiga-toxin (Stx) 2-positive strains such as *E. coli* O113 or O29 (Paton *et al.*, 2004; Morinaga *et al.*, 2007). Torgersen and colleagues reported that Stx is able to stimulate its own entry by a process dependent on the toxin concentration, the surface binding of the complete Stx and clathrin-dependent endocytosis (Torgersen *et al.*, 2005). On the other hand, macropinocytosis mediated through Src, non-muscle myosin II and cell division control 42 (Cdc42)-dependent mechanisms significantly increased Stx endocytosis by intestinal epithelial cells and stimulated toxin transcytosis (Malyukova *et al.*, 2009; Lukyanenko *et al.*, 2011). Romer and colleagues demonstrated that scission of Shiga toxin-induced tubular endocytic membrane invaginations is preceded by cholesterol-dependent membrane reorganization and dynamin-independent manner (Romer *et al.*, 2007; 2010). These findings suggest that Stx can invade the target cells using both receptor (Gb3)-mediated and receptor-independent mechanisms. Previously, our laboratory and other groups documented that SubAB was capable of binding to target cells expressing terminal sialic acid-modified membrane proteins (Yahiro *et al.*, 2006; 2011; Byres *et al.*, 2008). Although SubAB was internalized in Vero cells by clathrin-dependent endocytosis (Chong *et al.*, 2008), our findings show that SubAB uptake is dependent on lipid rafts and actin cytoskeleton, and independent of clathrin, caveolin and dynamin I/II pathways. Recent studies demonstrate that some proteins including prion protein utilized lipid raft-dependent macropinocytosis for internalization (Kruth *et al.*, 2005; Noguchi *et al.*, 2005; Wadia *et al.*, 2008). Thus, we conclude that SubAB uptake is by a lipid raft- and actin-dependent pathway in HeLa cells. Therefore, several mechanisms may participate in concert to facilitate SubAB uptake processing by target cells.

In conclusion, we demonstrate a new route of SubAB uptake by HeLa cells. Previous studies have been shown that SubAB induced severe inflammation in multiple organs and haemorrhage of the small intestine in mice (Wang *et al.*, 2007; Furukawa *et al.*, 2011). These pleiotropic effects of SubAB *in vivo* may result from its entry into target cells via different endocytic routes, including a clathrin or lipid raft-dependent route. Our study may lead to a novel therapeutic strategy to avoid severe organ damage in non-O157 STEC infection. Prevention of SubAB and Stx uptake by intestinal epithelial cells during infection with non-O157 STEC may block the harmful consequences of infection.

Experimental procedures

Cells culture and gene silencing

HeLa cells were cultured at 37°C in a humidified 5% CO_2 atmosphere in Eagle's minimum essential medium (EMEM) (Sigma) containing 10% heat-inactivated fetal bovine serum (FBS), 100 U ml^{-1} penicillin and 0.1 mg ml^{-1} streptomycin. RNA interference-mediated gene knockdown was performed using validated Qiagen HP small-interfering RNAs (siRNAs) for clathrin (SI299880), caveolin1 (SI00299642) and caveolin2 (SI02664389). Dynamin I/II siRNA (sc43736) was from Santa Cruz Biotechnology. PKCδ siRNAs (Llado *et al.*, 2004) were designed and validated as described previously. PAK1 siRNAs specific were purchased from Dharmacon (M-003521-04). Negative-control (NC) siRNAs were purchased from Sigma Aldrich or Dharmacon. HeLa cells were transfected with 100 nM of the indicated siRNAs for 48–72 h using LipofectamineTM RNAiMax transfection reagent (Invitrogen) according to the manufacturer's protocol. Transfection efficiency and effect were evaluated by Western blotting using the indicated antibodies.

Reagents

Pharmacological inhibitors were prepared either in water or DMSO following the manufacturer's recommendations and used at the indicated concentrations. Methyl-β-cyclodextrin (c45551G), Dynasore hydrate (D7693), Filipin III (F4767), ionomycin (I9657), cytochalasin D (C8273) and EGTA were from Sigma Aldrich; Chlorpromazine hydrochloride (ALX270171G001), 5-ethylisopropyl amiloride (ALX550266M005) and Rottlerin (ALX350075M010) from Enzo Life Science; and PI3K inhibitors, LY294002 (9901) and wortmannin (9951S) from Cell Signaling Technology. PAK inhibitor IPA-3 and Bafilomycin A1 were obtained from WAKO. For Western blot analysis, anti-BiP/GRP78 (610978), anti-clathrin (610499), anti-caveolin I (610406), anti-caveolin II (610684) and anti-PKCδ (610398) antibodies were purchased from Becton Dickinson, and anti-dynamin I/II antibody (2342) was from Cell Signaling Technology. These studies also utilized anti-GAPDH antibody from GeneTex (GTX100118); anti-PAK1 (Ab-212) antibody was from Signalway Antibody; and HRP-conjugated anti-rabbit IgG (7074) and anti-mouse IgG (7076) antibodies from R & D Systems. For immunofluorescence studies, anti-BiP/GRP78 antibodies (sc-1051) were purchased from Santa Cruz Biotechnology; Alexa Fluor® 488 donkey anti-goat IgG (A-11055), Alexa Fluor® 488 goat anti-mouse IgM and Alexa Fluor® 555 cholera toxin B subunit (CtxB) from Invitrogen; and anti-stain™ 488 Fluorescent phalloidin (PHDG1) from Cytoskeleton, Inc. Recombinant Hamster BiP/GRP78 (SR-C765) was from MBL. Isotonic Na^+-rich, K^+-rich, and NMG^+-rich buffers were prepared as described previously (Koivusalo *et al.*, 2010).

Preparation of subtilase cytotoxin

Recombinant His-tagged wild-type subtilase cytotoxin (SubAB) or catalytically inactivated mutant SubA (S272A)B (mSubAB) were synthesized in *E. coli* and purified by Ni-NTR chromatography as described previously (Morinaga *et al.*, 2007).

Western blot analysis

HeLa cells (1×10^5 cells per well) in a 24-well plate were cultured overnight in 500 μl of EMEM containing 10% FBS. After pretreatment with the indicated inhibitors for 30 min, cells were treated with SubAB (400 ng ml^{-1}) or mSubAB (400 ng ml^{-1}) for 1 h at 37°C. Cells were mixed with 100 μl of SDS-sample buffer (62.5 mM Tris pH 6.8, 1% SDS, 10% glycerol, 5 mM dithiothreitol, 0.001% bromophenol blue), and heated at 100°C for 5 min. After SDS-PAGE in 15% gels, proteins were transferred to Immobilon-P membranes (Millipore), which were incubated with primary antibodies for 1 h at room temperature or overnight at 4°C, then washed with TTBS three times, incubated with the appropriate HRP-linked secondary antibodies at room temperature for 1 h, washed with TTBS three times, and finally incubated in Super Signal West Pico mixture (Thermo Scientific). HRP-bound protein bands were visualized by Las-1000 (Fuji Film).

Internalization assays for SubAB, transferrin and FITC-Dextran

To investigate localization of SubAB in HeLa cells, SubAB was labelled with Alexa555 (Invitrogen) according to the instruction manual. Cells (3×10^5 cells per well) in a six-well dish were grown on glass coverslips overnight in EMEM containing 10% FBS and pretreated with the indicated inhibitors for 30 min at 37°C. After incubation with Alexa555-labelled SubAB (5 μg ml^{-1}) for 30 min at 4°C, cells were washed with PBS and incubated for 1 h at 37°C. After an additional wash with PBS, cells were fixed for 20 min with 4% paraformaldehyde, permeabilized for 5 min with 0.1% Triton X-100, and blocked with 4% Block-Ace buffer (Snow Bland) for 30 min. Cells were incubated with primary antibodies for 1 h at room temperature, washed with PBS, and then treated for 1 h at room temperature with secondary Alexa488-conjugated antibody. The washed coverslips were mounted in Prolong Gold and Slow Fade Gold Antifade Reagents (Invitrogen) and observed by confocal microscopy (Fluoview Fv10i, OLYMPUS). For transferrin uptake, cells were exposed to transferrin (Tf)-Alexa Fluor 488 (Life technology) for 15 min before fixation. For fluid-phase uptake, cells were exposed to 0.5 mg ml^{-1} FITC-dextran (SIGMA) for 10 min at 37°C before fixation at the indicated time points.

To examine further the localization of SubAB, the toxin was labelled with biotin according to the instruction manual, using EZ-Linksulfo-N-hydoroxylsulfosuccinimide-biotin (sulfo-NHS-SS-biotin) (Pierce) as described previously (Morinaga *et al.*, 2007). Briefly, HeLa cells (2×10^4 cells per well) were pretreated with the indicated concentrations of inhibitors for 30 min and then biotin-labelled SubAB was added for 1 h at 37°C after washing to remove unbound toxin. After 1 h, cells were washed, fixed and biotin bound to the cell surface was removed with 0.5 M 2-mercaptoethanesulfonic acid (MESNA); internalized biotin was detected following incubation with horseradish peroxidase (HRP)-conjugated streptavidin for 1 h, and then with its BM blue substrate (Roche Diagnostic Corp.). The reaction was stopped with 1 M H_2SO_4 and colour was measured at 450 nm. Background absorbance was subtracted.

Triton extraction

Triton X-100 extraction of HeLa cells cultured on coverslips was performed as described previously (Nichols *et al.*, 2001). After incubation with Alexa555-labelled SubAB or Alexa488-labelled Tf for 30 min at 37°C, cells were cooled to 4°C, incubated with cold 1% Triton X-100 in 50 mM Tris-HCl, 0.15 M NaCl pH7.7 for 20 min, then washed with cold PBS, and fixed with 4% paraformaldehyde.

BiP cleavage by SubAB in vitro

To investigate the direct effect of inhibitors on BiP cleavage by SubAB *in vitro* as described previously (Paton *et al.*, 2006), recombinant hamster BiP (0.1 μg per 10 μl) was incubated with SubAB (20 ng per 10 μl) in the presence or absence of the inhibitors. After 60 min incubation at 37°C, the samples were mixed with 10 μl of 2xSDS-sample buffer, and heated at 100°C for 5 min. After SDS-PAGE in 15% gels, BiP cleavage by SubAB was detected with anti-BiP antibody by Western blotting.

Acknowledgements

This work was supported by grants-in-aid for Scientific Research from the Ministry of Education, Science and Culture of Japan

(B-24390104), Improvement of Research Environment for Young Researchers from Japan Science and Technology Agency and grant-in-aids from the Ministry of Health, Labour and Welfare of Japan (H24-Shinkou-Ippan-012). Joel Moss was supported by the Intramural Research Program, National Institutes of Health and National Heart, Lung, and Blood Institute. We acknowledge the expert technical assistance of K. Hirano and A. Kiuchi.

References

Boquet, P., and Ricci, V. (2012) Intoxication strategy of *Helicobacter pylori* VacA toxin. *Trends Microbiol* **20:** 165–174.

Byres, E., Paton, A.W., Paton, J.C., Lofling, J.C., Smith, D.F., Wilce, M.C., *et al.* (2008) Incorporation of a non-human glycan mediates human susceptibility to a bacterial toxin. *Nature* **456:** 648–652.

Chong, D.C., Paton, J.C., Thorpe, C.M., and Paton, A.W. (2008) Clathrin-dependent trafficking of subtilase cytotoxin, a novel AB5 toxin that targets the endoplasmic reticulum chaperone BiP. *Cell Microbiol* **10:** 795–806.

Dharmawardhane, S., Schurmann, A., Sells, M.A., Chernoff, J., Schmid, S.L., and Bokoch, G.M. (2000) Regulation of macropinocytosis by p21-activated kinase-1. *Mol Biol Cell* **11:** 3341–3352.

Doherty, G.J., and McMahon, H.T. (2009) Mechanisms of endocytosis. *Annu Rev Biochem* **78:** 857–902.

Eash, S., Querbes, W., and Atwood, W.J. (2004) Infection of vero cells by BK virus is dependent on caveolae. *J Virol* **78:** 11583–11590.

Falcone, S., Cocucci, E., Podini, P., Kirchhausen, T., Clementi, E., and Meldolesi, J. (2006) Macropinocytosis: regulated coordination of endocytic and exocytic membrane traffic events. *J Cell Sci* **119:** 4758–4769.

Ferguson, S.M., Raimondi, A., Paradise, S., Shen, H., Mesaki, K., Ferguson, A., *et al.* (2009) Coordinated actions of actin and BAR proteins upstream of dynamin at endocytic clathrin-coated pits. *Dev Cell* **17:** 811–822.

Fretz, M., Jin, J., Conibere, R., Penning, N.A., Al-Taei, S., Storm, G., *et al.* (2006) Effects of Na+/H+exchanger inhibitors on subcellular localisation of endocytic organelles and intracellular dynamics of protein transduction domains HIV-TAT peptide and octaarginine. *J Control Release* **116:** 247–254.

Furukawa, T., Yahiro, K., Tsuji, A.B., Terasaki, Y., Morinaga, N., Miyazaki, M., *et al.* (2011) Fatal hemorrhage induced by subtilase cytotoxin from Shiga-toxigenic *Escherichia coli*. *Microb Pathog* **50:** 159–167.

Gruenberg, J., and van der Goot, F.G. (2006) Mechanisms of pathogen entry through the endosomal compartments. *Nat Rev Mol Cell Biol* **7:** 495–504.

Harper, C.B., Popoff, M.R., McCluskey, A., Robinson, P.J., and Meunier, F.A. (2013) Targeting membrane trafficking in infection prophylaxis: dynamin inhibitors. *Trends Cell Biol* **23:** 90–101.

Henley, J.R., Krueger, E.W., Oswald, B.J., and McNiven, M.A. (1998) Dynamin-mediated internalization of caveolae. *J Cell Biol* **141:** 85–99.

Hommelgaard, A.M., Roepstorff, K., Vilhardt, F., Torgersen, M.L., Sandvig, K., and van Deurs, B. (2005) Caveolae: stable membrane domains with a potential for internalization. *Traffic* **6:** 720–724.

Howes, M.T., Kirkham, M., Riches, J., Cortese, K., Walser, P.J., Simpson, F., *et al.* (2010) Clathrin-independent carriers form a high capacity endocytic sorting system at the leading edge of migrating cells. *J Cell Biol* **190:** 675–691.

Jiang, M., and Chen, G. (2009) Ca2+ regulation of dynamin-independent endocytosis in cortical astrocytes. *J Neurosci* **29:** 8063–8074.

Kagan, J.C., Su, T., Horng, T., Chow, A., Akira, S., and Medzhitov, R. (2008) TRAM couples endocytosis of Toll-like receptor 4 to the induction of interferon-beta. *Nat Immunol* **9:** 361–368.

Kalin, S., Amstutz, B., Gastaldelli, M., Wolfrum, N., Boucke, K., Havenga, M., *et al.* (2010) Macropinocytotic uptake and infection of human epithelial cells with species B2 adenovirus type 35. *J Virol* **84:** 5336–5350.

Koivusalo, M., Welch, C., Hayashi, H., Scott, C.C., Kim, M., Alexander, T., *et al.* (2010) Amiloride inhibits macropinocytosis by lowering submembranous pH and preventing Rac1 and Cdc42 signaling. *J Cell Biol* **188:** 547–563.

Kruth, H.S., Jones, N.L., Huang, W., Zhao, B., Ishii, I., Chang, J., *et al.* (2005) Macropinocytosis is the endocytic pathway that mediates macrophage foam cell formation with native low density lipoprotein. *J Biol Chem* **280:** 2352–2360.

Krzyzaniak, M.A., Zumstein, M.T., Gerez, J.A., Picotti, P., and Helenius, A. (2013) Host cell entry of respiratory syncytial virus involves macropinocytosis followed by proteolytic activation of the F protein. *PLoS Pathog* **9:** e1003309.

Kumari, S., Mg, S., and Mayor, S. (2010) Endocytosis unplugged: multiple ways to enter the cell. *Cell Res* **20:** 256–275.

Lajoie, P., Kojic, L.D., Nim, S., Li, L., Dennis, J.W., and Nabi, I.R. (2009) Caveolin-1 regulation of dynamin-dependent, raft-mediated endocytosis of cholera toxin-B sub-unit occurs independently of caveolae. *J Cell Mol Med* **13:** 3218–3225.

Llado, A., Tebar, F., Calvo, M., Moreto, J., Sorkin, A., and Enrich, C. (2004) Protein kinaseCdelta-calmodulin cross-talk regulates epidermal growth factor receptor exit from early endosomes. *Mol Biol Cell* **15:** 4877–4891.

Lukyanenko, V., Malyukova, I., Hubbard, A., Delannoy, M., Boedeker, E., Zhu, C., *et al.* (2011) Enterohemorrhagic *Escherichia coli* infection stimulates Shiga toxin 1 macropinocytosis and transcytosis across intestinal epithelial cells. *Am J Physiol Cell Physiol* **301:** C1140–C1149.

Macia, E., Ehrlich, M., Massol, R., Boucrot, E., Brunner, C., and Kirchhausen, T. (2006) Dynasore, a cell-permeable inhibitor of dynamin. *Dev Cell* **10:** 839–850.

McMahon, H.T., and Boucrot, E. (2011) Molecular mechanism and physiological functions of clathrin-mediated endocytosis. *Nat Rev Mol Cell Biol* **12:** 517–533.

Malyukova, I., Murray, K.F., Zhu, C., Boedeker, E., Kane, A., Patterson, K., *et al.* (2009) Macropinocytosis in Shiga toxin 1 uptake by human intestinal epithelial cells and transcellular transcytosis. *Am J Physiol Gastrointest Liver Physiol* **296:** G78–G92.

Mercer, J., and Helenius, A. (2008) Vaccinia virus uses macropinocytosis and apoptotic mimicry to enter host cells. *Science* **320:** 531–535.

Mercer, J., and Helenius, A. (2009) Virus entry by macropinocytosis. *Nat Cell Biol* **11:** 510–520.

Mercer, J., Knebel, S., Schmidt, F.I., Crouse, J., Burkard, C., and Helenius, A. (2010) Vaccinia virus strains use distinct forms of macropinocytosis for host-cell entry. *Proc Natl Acad Sci USA* **107:** 9346–9351.

Mesaki, K., Tanabe, K., Obayashi, M., Oe, N., and Takei, K. (2011) Fission of tubular endosomes triggers endosomal acidification and movement. *PLoS ONE* **6:** e19764.

Morinaga, N., Yahiro, K., Matsuura, G., Watanabe, M., Nomura, F., Moss, J., and Noda, M. (2007) Two distinct cytotoxic activities of subtilase cytotoxin produced by shiga-toxigenic *Escherichia coli*. *Infect Immun* **75:** 488–496.

Nabi, I.R., and Le, P.U. (2003) Caveolae/raft-dependent endocytosis. *J Cell Biol* **161:** 673–677.

Nichols, B.J., Kenworthy, A.K., Polishchuk, R.S., Lodge, R., Roberts, T.H., Hirschberg, K., *et al.* (2001) Rapid cycling of lipid raft markers between the cell surface and Golgi complex. *J Cell Biol* **153:** 529–541.

Noguchi, H., Matsumoto, S., Okitsu, T., Iwanaga, Y., Yonekawa, Y., Nagata, H., *et al.* (2005) PDX-1 protein is internalized by lipid raft-dependent macropinocytosis. *Cell Transplant* **14:** 637–645.

Nonnenmacher, M., and Weber, T. (2011) Adeno-associated virus 2 infection requires endocytosis through the CLIC/GEEC pathway. *Cell Host Microbe* **10:** 563–576.

Orlandi, P.A., and Fishman, P.H. (1998) Filipin-dependent inhibition of cholera toxin: evidence for toxin internalization and activation through caveolae-like domains. *J Cell Biol* **141:** 905–915.

Park, R.J., Shen, H., Liu, L., Liu, X., Ferguson, S.M., and De Camilli, P. (2013) Dynamin triple knockout cells reveal off target effects of commonly used dynamin inhibitors. *J Cell Sci* **126:** 5305–5312.

Paton, A.W., Srimanote, P., Talbot, U.M., Wang, H., and Paton, J.C. (2004) A new family of potent AB(5) cytotoxins produced by Shiga toxigenic *Escherichia coli*. *J Exp Med* **200:** 35–46.

Paton, A.W., Beddoe, T., Thorpe, C.M., Whisstock, J.C., Wilce, M.C., Rossjohn, J., *et al.* (2006) AB5 subtilase cytotoxin inactivates the endoplasmic reticulum chaperone BiP. *Nature* **443:** 548–552.

Romer, W., Berland, L., Chambon, V., Gaus, K., Windschiegl, B., Tenza, D., *et al.* (2007) Shiga toxin induces tubular membrane invaginations for its uptake into cells. *Nature* **450:** 670–675.

Romer, W., Pontani, L.L., Sorre, B., Rentero, C., Berland, L., Chambon, V., *et al.* (2010) Actin dynamics drive membrane reorganization and scission in clathrin-independent endocytosis. *Cell* **140:** 540–553.

Sanchez, E.G., Quintas, A., Perez-Nunez, D., Nogal, M., Barroso, S., Carrascosa, A.L., and Revilla, Y. (2012) African swine fever virus uses macropinocytosis to enter host cells. *PLoS Pathog* **8:** e1002754.

Sanchez, E.G., Quintas, A., Nogal, M., Castello, A., and Revilla, Y. (2013) African swine fever virus controls the host transcription and cellular machinery of protein synthesis. *Virus Res* **173:** 58–75.

Sieczkarski, S.B., and Whittaker, G.R. (2002) Dissecting virus entry via endocytosis. *J Gen Virol* **83:** 1535–1545.

Smith, R.D., Willett, R., Kudlyk, T., Pokrovskaya, I., Paton, A.W., Paton, J.C., and Lupashin, V.V. (2009) The COG complex, Rab6 and COPI define a novel Golgi retrograde trafficking pathway that is exploited by SubAB toxin. *Traffic* **10:** 1502–1517.

Soltoff, S.P. (2007) Rottlerin: an inappropriate and ineffective inhibitor of PKCdelta. *Trends Pharmacol Sci* **28:** 453–458.

Toni, M., Spisni, E., Griffoni, C., Santi, S., Riccio, M., Lenaz, P., and Tomasi, V. (2006) Cellular prion protein and caveolin-1 interaction in a neuronal cell line precedes Fyn/Erk 1/2 signal transduction. *J Biomed Biotechnol* **2006:** 69469.

Torgersen, M.L., Lauvrak, S.U., and Sandvig, K. (2005) The A-subunit of surface-bound Shiga toxin stimulates clathrin-dependent uptake of the toxin. *FEBS J* **272:** 4103–4113.

Tsutsuki, H., Yahiro, K., Suzuki, K., Suto, A., Ogura, K., Nagasawa, S., *et al.* (2012) Subtilase cytotoxin enhances *Escherichia coli* survival in macrophages by suppression of nitric oxide production through the inhibition of NF-kappaB activation. *Infect Immun* **80:** 3939–3951.

Viaud, J., and Peterson, J.R. (2009) An allosteric kinase inhibitor binds the p21-activated kinase autoregulatory domain covalently. *Mol Cancer Ther* **8:** 2559–2565.

de Vries, E., Tscherne, D.M., Wienholts, M.J., Cobos-Jimenez, V., Scholte, F., Garcia-Sastre, A., *et al.* (2011) Dissection of the influenza A virus endocytic routes reveals macropinocytosis as an alternative entry pathway. *PLoS Pathog* **7:** e1001329.

Wadia, J.S., Stan, R.V., and Dowdy, S.F. (2004) Transducible TAT-HA fusogenic peptide enhances escape of TAT-fusion proteins after lipid raft macropinocytosis. *Nat Med* **10:** 310–315.

Wadia, J.S., Schaller, M., Williamson, R.A., and Dowdy, S.F. (2008) Pathologic prion protein infects cells by lipid-raft dependent macropinocytosis. *PLoS ONE* **3:** e3314.

Wang, H., Paton, J.C., and Paton, A.W. (2007) Pathologic changes in mice induced by subtilase cytotoxin, a potent new *Escherichia coli* AB5 toxin that targets the endoplasmic reticulum. *J Infect Dis* **196:** 1093–1101.

Wang, X., Kleyman, T.R., Tohda, H., Marunaka, Y., and O'Brodovich, H. (1993) 5-(N-Ethyl-N-isopropyl)amiloride sensitive Na+ currents in intact fetal distal lung epithelial cells. *Can J Physiol Pharmacol* **71:** 58–62.

Williamson, L.C., and Neale, E.A. (1994) Bafilomycin A1 inhibits the action of tetanus toxin in spinal cord neurons in cell culture. *J Neurochem* **63:** 2342–2345.

Yahiro, K., Morinaga, N., Satoh, M., Matsuura, G., Tomonaga, T., Nomura, F., *et al.* (2006) Identification and characterization of receptors for vacuolating activity of subtilase cytotoxin. *Mol Microbiol* **62:** 480–490.

Yahiro, K., Satoh, M., Morinaga, N., Tsutsuki, H., Ogura, K., Nagasawa, S., *et al.* (2011) Identification of subtilase cytotoxin (SubAB) receptors whose signaling, in association with SubAB-induced BiP cleavage, is responsible for apoptosis in HeLa cells. *Infect Immun* **79:** 617–627.

Yahiro, K., Tsutsuki, H., Ogura, K., Nagasawa, S., Moss, J., and Noda, M. (2012) Regulation of subtilase cytotoxin-induced cell death by an RNA-dependent protein kinase-like endoplasmic reticulum kinase-dependent proteasome pathway in HeLa cells. *Infect Immun* **80:** 1803–1814.

Supporting information

Additional Supporting Information may be found in the online version of this article at the publisher's web-site:

Fig. S1. Analysis of SubAB uptake.

A. HeLa cells were incubated with Alexa555-labelled SubAB (red) for 1 h at 4°C or 37°C. Cells were fixed and reacted with anti-BiP antibodies (green) and then analysed by serial *z*-stack images by confocal microscopy. Experiments were repeated at least three times with similar results.

B. Cells were pretreated with the indicated inhibitors [e.g. 80 μM Dynasore (Dyna), 40 μg ml^{-1} CPZ, 10 mM mβCD, 100 μM EIPA, 0.5 μM Bafilomycin A1 (Baf A1), 40 μM LY294002 (LY), 200 nM wortmannin (Wort), 25 μM BAPTA-AM (BAPTA), and 10 μM cytochalasin D (Cyt D)] for 30 min and then biotin-labelled SubAB was added for 1 h at 37°C. Cells were fixed and biotin bound to the cell surface was removed with MESNA; internalized biotin was quantified as in *Experimental procedures*. The relative activities of biotin-labeled SubAB uptake in HeLa cells were set as 1, and the values of other groups were standardized against it. The total binding to HeLa cells was 3.558 ± 0.35. Data are the means ± SD of values from three independent experiments with triplicate wells. $^*P < 0.05$.

Fig. S2. Effect of Rottlerin on SubAB-mediated BiP cleavage.

A. HeLa cells were pretreated with the indicated concentrations of Rottlerin for 30 min, and then cells were treated with mt or wt SubAB for 1 h and analysed by Western blot with the indicated antibodies (left panel). Quantification of uncleaved BiP (78 kDa) following incubation with mt or wt SubAB in the presence of the indicated inhibitors was performed by densitometry (right panel). Data are the means ± SD from three independent experiments. $^*P < 0.05$.

B. Cells were pretreated with 40 μM Rottlerin for 30 min and then incubated with Alexa555-labelled SubAB for 1 h at 37°C. Cells were imaged by confocal microscopy for colocalization of SubAB (red) with BiP (green) as described in *Experimental procedures*. Bars represent 20 μm. Experiments were repeated two times with similar results (bottom).

C. HeLa cells were transfected with control (NC) or PKCδ siRNA, and cell lysates were subjected to immunoblotting with the indicated antibodies. GAPDH served as a loading control. Quantification by densitometry of the amounts of PKCδ (78 kDa) with knockdown by the indicated siRNA. Experiments were repeated three times with similar results. Data are the means ± SD from three separate experiments. $^*P < 0.05$.

Fig. S3. Effect of inhibitors on SubAB-mediated BiP cleavage *in vitro*.

Recombinant hamster BiP (0.1 μg per 10 μl) was incubated with SubAB (20 ng per 10 μl) in the presence or absence of the indicated inhibitors. The concentration of the inhibitors was 80 μM Dynasore (Dyna), 40 μg ml^{-1} CPZ, 300 μM MCD, 40 μM LY294002 (LY), 200 nM wortmannin (Wort), 25 μM BAPTA-AM (BAPTA), 100 μM EIPA, 40 μM Rottlerin (Rot) and 10 μM cytochalasin D (Cyt D). After 60 min incubation at 37°C, the samples were mixed with 10 μl of 2xSDS-sample buffer, and heated at 100°C for 5 min. After SDS-PAGE in 15% gels, BiP cleavage by SubAB was detected with anti-BiP antibody by Western blotting. Experiments were repeated three times with similar results.

溶血性尿毒症症候群の診断・治療ガイドライン

総括責任者
五十嵐　隆
国立成育医療研究センター総長

編集
溶血性尿毒症症候群の診断・治療ガイドライン作成班

東京医学社

溶血性尿毒症症候群の診断・治療ガイドライン作成班班員

総括責任者：	五十嵐　隆	（国立成育医療研究センター総長）
分担研究者：	齋藤　昭彦	（新潟大学医学部小児科教授）
	伊藤　秀一	（国立成育医療研究センター腎臓・リウマチ・膠原病科医長）
	幡谷　浩史	（東京都立小児総合医療センター腎臓内科医長）
	水口　　雅	（東京大学大学院医学系研究科国際保健学教授）
	森島　恒雄	（岡山大学医学部小児科教授）
研究協力者：	大西　健児	（東京都立墨東病院感染症科部長）
	川村　尚久	（大阪労災病院小児科部長）
	北山　浩嗣	（静岡県立こども病院腎臓科医長）
	芦田　　明	（大阪医科大学小児科講師）
	要　　伸也	（杏林大学医学部第一内科准教授）
	種市　尋宙	（富山大学医学部小児科助教）
	佐古まゆみ	（国立成育医療研究センター臨床試験推進室）

溶血性尿毒症症候群の診断・治療ガイドライン　査読委員

服部　元史	（東京女子医科大学腎臓総合医療センター腎臓小児科教授）
本田　雅敬	（東京都立小児総合医療センター副院長）
石倉　健司	（東京都立小児総合医療センター腎臓内科医長）
小林　信秋	（認定ＮＰＯ法人難病のこども支援全国ネットワーク）

本ガイドライン作成班班員の利益相反事項の開示について

本ガイドラインを作成した平成 24 年度に，作成班班員の五十嵐隆，伊藤秀一，幡谷浩史，水口雅，森島恒雄，大西健児，北山浩嗣，芦田明，要伸也，種市尋宙，佐古まゆみは，日本小児科学会，日本小児腎臓病学会，日本腎臓学会が定める論文公表時の利益相反開示事項に該当する項目がなかった．また，作成班班員の齋藤昭彦はファイザー株式会社，MSD，田辺三菱製薬からの講演料が，川村尚久はグラクソ・スミスクライン株式会社からの研究費と，ジャパン・ワクチン株式会社とグラクソ・スミスクライン株式会社からの講演料が，日本小児科学会，日本小児腎臓病学会，日本腎臓学会が定める論文公表時の利益相反開示事項に該当していた．